SKA - Paris 01 Sept 2006

SURVEYS, CALIBRATION and IMAGING

Melvyn Wright (University of California, Berkeley), Jaap Bregman (ASTRON), Robert Braun (ASTRON), John Bunton (CSIRO), Tim Cornwell (CSIRO), Ron Ekers (CSIRO), Bryan Gaensler (CFA), Peter Hall (SKA-ISPO), Colin Lonsdale (Haystack), John O'Sullivan (CSIRO), Nan Rendong (Beijing), Richard Schilizzi (SKA-ISPO), Russ Taylor (Calgary)

SKA Task Force on Survey optimization

1. ABSTRACT

• Surveys require low frequency, low resolution images

• Stringent requirements on calibration at every stage of beam formation.

• Computing cost strongly depends on calibration and science requirements.

• Calibration requirements set by confusion from strong sources.

• Imaging and Calibration intimately related.

• SKA design must include overall system from science goals to data products.

• Calibration and Imaging can be integrated with DSP hardware.

– Stream data processing

– Calibration in real time using global model.

– Calibration feedback into beam formers and imagers.

– Simultaneous imaging at multiple phase centers.

– Calibrated images as normal output from SKA.

2. SCIENCE GOALS

• 60% of Key Science projects require all-sky or 1000 sq deg surveys.

• All are below 2 GHz, with a useful range extending to 3 GHz.

– Four pulsar surveys are in range 1-2 GHz.

– Dark Energy HI survey 0.5-1 GHz.

– Evolution of gas in galaxies 0.2-1.4 GHz.

– All sky 1 micro Jy survey 1.4 GHz.

– EOR all-sky HI survey from z=19 to z=6 at 70-200 MHz.

• Instantaneous FOV

– 1-10 sq deg, except Dark Energy which requires 50 sq deg.

– FOV can often be traded for sensitivity.

– Full sensitivity of SKA required with limited FOV for some KSPs.

– Dark Energy needs large FOV at full sensitivity so no room to trade.

– Intrinsic properties of sources can be used to reduce confusion.

• Array configuration

– Maximum baselines range from 1 to 200 km.

– Four surveys require only compact core within 1-5 km

• Dynamic range, Calibration and Confusion.

– Two Key Science projects require image dynamic range 10^7.

– Imaging HI requires continuum subtraction to avoid confusion limit.

– Polarization surveys require calibration across FOV and bandwidth.

– Calibration is essential to achieve science goals.

• Need closer interaction between astronomers and engineers.

3. ARRAY OPTIMIZATION

• Survey speed $\sim FOV \times (A/T)^2 \times BW$ ——————(1)

• For LNSD-FPA, $FOV \sim N_{beams} \times (\lambda/D)^2$, and $A \sim ND^2$, then,

• Survey speed $\sim N_{beams} \times \lambda^2 \times (ND/T)^2 \times BW$ ——————(2)

• For PAFs, maximum $N_{beams} \sim 1/\lambda^2$, Survey speed $\sim$ PAF area.

– the useful BW and N_{beams} are defined by the science goals.

– ND dependence for regions larger than the antenna FOV.

• Regions < FOV of antenna need only one beam, then,

SKA Sensitivity $\sim (ND^2/T)^2 \times BW$ ——————————(3)

• Mosaics are required if region larger than $N_{beams} \times (\lambda/D)^2$.

– 5m antenna with a single feed has $\sim$ 50 sq deg instantaneous FOV at 500 MHz.

– Single feeds, MFCs and PAFs needed for full frequency range of the SKA.

4. ANTENNAS

• Cost scales as $D^{2+x}\lambda^{-y}$; where $0 < [x, y] < 1$

• Antenna primary beam pattern attenuates radiation from outside the FOV.

• Primary beam calibration limits dynamic range of uvdata.

• Primary beam and pointing errors limit image fidelity in mosaics.

– stable primary beams require fewer parameters for calibration.

– antennas engineered for 25 GHz are more stable for low freq surveys.

• Sidelobe structure of primary beam outside FOV increases confusion noise.

• Spillover past reflecting surfaces increases Tsys.

• Cross talk from nearby antennas gives false correlations.

– careful design of scattering surfaces on antennas can reduce this problem.

• Offset antenna design

– reduces aperture blockage,

– reduces scattering,

– costs more

– increases the minimum antenna separation (mosaicing).

• Equatorial mount

– feed leg diffraction pattern fixed on sky.

– costs more

5. RECEIVERS

• Cost is function of the complexity of the receiver.

– feeds, LNA, cyrogenics, FPAs and phasing electronics.

– cyrogenics lower T_{sys} at high frequencies, but are major operational cost.

• Pulsar timing, Dark energy require full on axis sensitivity.

– trading FOV for A/T decreases the capability of the SKA.

5.1. Array Receivers - MCFs

• Focal plane array receivers can provide multiple beams for surveying.

– MCFs must be spaced by $> \lambda$ for efficient illumination.

– interleaved observations required to fully sample for surveying.

5.2. Phased Array Receivers - PAFs

• PAF receptors spaced by $< \lambda$ avoids grating lobes, λ at shortest wavelength.

– PAFs can fully sample the sky.

– number of receivers per beam from $\sim$ 2.4 to 3.3 as the PAF gets smaller.

– T_{sys} for PAF receivers higher than cooled MFC at L-band.

– can correct for off-axis aberrations, aperture blockage, and aperture surface

– corrections require accurate calibration of PAF receiver elements.

• Focal plane arrays have obvious science and engineering appeal.

– Re-use expensive collecting area.

– Frequency independent, wide FOV.

5.3. Risk, Receivers and RFI

• FPAs are a good strategy if one already has large expensive antennas.

– PAF can correct large scale errors in aperture surface at cost of additional calibration parameters and computational load.

• Large apertures with FPA receivers for SKA ?

– exchange of collecting area for FPA receivers compromises non-survey science.

– transfers resources from collecting area into higher risk design and electronics.

• High aperture efficiencies can be obtained using phase array receivers.

– high efficiency implies high coupling between beams.

– Stein efficiency: forward gain related to coupling between phased array beams.

• Sidelobes of one phased array beam appear in direction of other beams at a level $\sim 1/N_{rec}$ where N_{rec} is the number of receiver elements.

– Coupling between beams reduced by re-weighting phased array, but costs forward gain, and higher sidelobes.

• Moores law drives down the cost of electronics, so spend less on antennas.

– Corollary: electronics become obsolete, better to invest in antennas and infrastructure with longer lifetimes, and treat receivers as upgrade path as the SKA is built.

• RFI generated by high speed digital electronics on antennas must be carefully shielded. 100 db isolation may be required to avoid correlated clock frequencies and switching harmonics.

– Alternatively, digital logic to support FPA receivers can be connected by fiber to multiple layers of RFI secure cages away from the receiver elements.

6. SIGNAL PROCESSING, STATIONS and ARRAY CONFIGURATION

• Digitizers and DSP bring data from antennas to beam formers and correlators.

– compact stations reduce data transport costs,

– computing costs increase if the uv-coverage is inadequate.

• Array configuration is defined by the science requirements.

– surveys compare images at different frequencies.

– sharp transition from central core into sparse distribution gives frequency dependent uv-coverage which is not optimum for comparing surveys at different frequencies.

• quality of images limited by the uv-coverage.

– optimize the antenna configuration.

– similar uv-coverage over wide range of frequencies

• Frequency dependent shortest uv-spacings are a problem

– short spacings from mosaicing and single dish observations.

• Antennas can be distributed in fractal network with fibers branching to individual antennas from nodes.

– fiber to antenna cluster 100 km from central core is similar for station diameter 100m or a few km if land acquisition costs are low.

– at larger radii antennas clustered; uv-coverage by earth rotation.

– correlations of antennas in central core with cluster at larger radii samples a broad swath in uv-plane.

7. BEAM FORMERS

• Phased array beams can be formed anywhere in sky by adding voltages in phase from subsets of antennas.

– sidelobes structure of each beam depends on array geometry, source direction, and weighting of signals from each antenna.

– beam formation is appropriate for analyzing signals from discrete radio sources such as pulsars, SETI targets and RFI sources.

– beam formation allows us to channel collecting area of large arrays into expensive back end analysis engines.

– imaging using beam formation is appropriate for compact sources, but is currently too expensive for imaging large fields.

• Beam formers can be used to reduce the data rate into correlators.

– time dependent calibration of beam formers can be obtained using correlators.

• Beam formation is a powerful construct, but has the "problem" that it phases up the signals from multiple receptors and the original information of the wavefront propagation to each receptor is lost.

– not quite lost, for it is possible, but expensive, to recover some information in post-processing.

– beamformer phasing varies with time, frequency, and direction in the sky.

– we phase up the beamformer in the desired direction, but the response is to sources over the whole sky.

• In order to subtract a strong source in the sidelobes we need to know the calibration in that direction.

– survey science requirements for this calibration are specified by the dynamic range required to avoid being confusion limited.

– dynamic range requirements are greatly reduced when intrinsic properties of the sources, e.g. time (pulsars), frequency (narrow lines) or compact size, allow discrimination against confusing sources.

– statistical properties of expected line emission (HI in clusters, EOR) may help discriminate against confusion from continuum sources in time and frequency dependent sidelobes.

• Dynamic range requirement for continuum emission $\sim 10^{6-7}$ for confusion from a 100 mJy source within a 1 sq deg FOV at 1.4 GHz (Thompson).

– 100 Jy sources in 10^{-3} sidelobes and 10 Jy sources in 1% sidelobes give comparable confusion level.

• Calibration errors of beam formers in direction of each source create sidelobes which raise noise floor.

– dynamic range can be estimated from amplitude and phase errors in beam former calibration.

– for random errors, dynamic range $\sim N/\epsilon$, where N is number of antennas in station beam or number of receptors in focal plane array receiver beam, and ϵ is error at each antenna or receptor.

• We rely on sidelobe suppression and calibration of beam formation to achieve the dynamic range required.

– Cornwell lists five levels of beam formation: Antenna, FPA, Station, Array, and Time-Bandwidth averaging.

– low resolution surveys (EOR, HI), do not allow much Time-Bandwidth averaging.

• We must calibrate each level of beam formation. Errors in these calibrations increase coupling between beams which throws an extra burden on data processing.

– for RF beam formers in aperture array tiles there is no calibration at all.

– in station made from a set of tiles we need station calibration to find the electronic gains that need to be corrected with an appropriate weight in the digital beam former.

– once all the tile signals are added to provide a station beam the effect of a wrong weight of a tile in a station is an error in the correlations made between stations.

– same is true for the beam former in a PAF; the signals from receptor elements in FPA receiver can be combined to form multiple beams in different directions. The signals from these beams are correlated with the corresponding beams from other telescopes.

– wrong weight in a PAF beam former is an error in correlations between PAF beams.

– subsequent modeling in self-calibration could include some parameters to correct for actual shape of station and PAF beams.

– complete parametrization could include all the weights for the corresponding elements of an aperture array or FPA receiver.

– shaping the edge illumination to minimize far out sidelobes or null steering for interferers may need further information.

• Calibration in close to real time to reduce cost and data handling in off-line data processing.

– implies measurements with sufficient parameters and SNR to calibrate with accuracy and time scales required.

– we must design systems and observing strategies to do this.

– hierarchical calibration may be possible.

– correlation of individual receptors with phased up signal may be needed to obtain sufficient SNR on the time scales required.

– phased up signal for subset of array could be routed back to each array antenna to provide a reference.

– correlator or other DSP is then required at each antenna to derive this calibration.

– RFI from DSP hardware at the antenna must be extremely well shielded.

• Alternatively the correlation can be part of centralized real time calibration hardware, on a time and computing resource shared basis.

– data bandwidth from each station is similar if N_{beams} are formed from N phased array receivers or from N antennas at the station, or in centralized (well shielded) DSP and computing nodes.

– see the beam former in Fig 1

– time resolution required for calibration varies from slow antenna surface deformations to fast, $\sim$ 1–10 sec atmospheric phase fluctuations.

• Beam formers can provide some suppression of interfering sources.

– complex gains are applied to elements of beam former (station antennas, or PAF receptors) to form nulls in directions of interfering sources.

– multiple nulls can be placed to form extended nulls or to attenuate widely separated RFI or confusing sources.

– calibration errors degrade the null.

– gains may need to be updated on 100 ms time scales.

– SNR at phase center is a function of number of nulls and number of elements in beam former. SNR $\sim$ 1 - $N_{nulls}/(2N_{ants} - N_{nulls} - 2)$.

• For the highest dynamic range the calibration implicit in beamforming with FPA or station beams must be redone in the data analysis, and leads to a large increase in computing costs.

– closing calibration loop at end of data reduction (i.e. full selfcalibration) probably only needed for continuum or small number of averaged channels so computing substantially less than making images for separate channels.

– need to quickly image using time variable primary beams. Making corrections in the gridding is one way.

8. CORRELATORS

• Cross correlation of all antennas provides complete sampling of incident wavefront.

– allows imaging full FOV of the individual antennas.

– versatile mechanism for integrating data in *uv* domain.

– 40 years of development calibrating and imaging using *uv* data.

• Current technology allows construction of GHz bandwidth correlators for arrays of 1000's of antennas

– extrapolating existing radio astronomy correlators: 4000 antenna, 1 GHz bandwidth correlator is reasonable by 2020.

– cost is a few percent of the SKA.

• The current plan is to correlate the inner $\sim$ 2000 antennas, and to correlate phased stations at longer baselines.

– large correlator needed to correlate 1000's of antennas, and high data rates are both seen as problems.

– early fears that correlation of all antennas was not achievable are no longer a major concern.

– recent developments have solved N^2 and connectivity for large-N arrays.

• Strawman design with correlations between stations of phased antennas presents significant problems:

– Fourier plane is less well sampled leading to high sidelobe level in synthesized array beams.

– high sidelobe level increases data processing required by N_{sta}, the number of antennas per station.

– station beams form primary beam pattern for array beams.

– station beam has a sidelobe level $\sim 1/N_{sta}$.

– each station beam different, depending on geometry and weighting.

– station beam time variable due to projection geometry, interference mitigation, antenna failures and calibration errors.

• correlations between stations of phased antennas degrade both primary beam, and synthesized array beam.

– e.g. $\sim$ 4000 antennas, $\sim$ 64 stations each with $\sim$ 64 antennas gives sidelobe level $\sim$ 1.6% in both station and array beams.

– dynamic range 10^6 and image fidelity 10^4 may not be possible using correlations between station beams.

• Correlation of all antennas is now possible.

– cost of correlators has come down and techniques of building large N correlators have been solved; this appears to provide a good solution for the SKA.

– correlation provides calibration at every level of beam formation.

– we don't have to cross correlate all receptors all the time, but must calibrate wavefront into station beams and FPAs.

– calibration varies with time, frequency, and direction in sky.

• More correlated antennas, means more parameters to determine the calibration, and better imaging properties.

9. CALIBRATION

• A-priori model used for calibration and imaging.

– in standard paradigm, strong compact sources are primary calibrators

– self-calibration is used during off-line imaging.

• Model visibility

$V'_{j,k} = exp(2\pi i/\lambda\ r.s_0) \times \Sigma(I \times A \times B \times P \times G \times \exp(2\pi i/\lambda\ r.(s - s_o))$

– $I(s, \nu, p)$ is the model image,

– $A(s, \nu, p)$ is the primary beam response,

– $B(\nu)$ is the instrumental bandpass,

– $P(s, \nu, p)$ is the polarization calibration,

– $G(t, s_0)$ is the gain versus time and phase center.

– $r = (r_j - r_k)$ is the baseline vector, and

– s, ν, and p are the position, frequency and polarization.

– s_o is the phase center for each region of interest.

• Problems:

– Primary beam, $A(s, \nu, p)$, is product of the antenna voltage patterns.

– Station beams vary with geometry and atmospheric fluctuations.

– Sources outside FoV must be subtracted to achieve high image fidelity.

– Confusing sources in different isoplanatic regions.

– Deconvolution is a major expense in the computation.

9.1. Calibration Data Processing

• Separately calibrate each phase center.

– identify bright emission from a-priori images

– image regions which are of interest.

– image sources whose sidelobes corrupt the regions of interest.

• Integrate data at each phase center. (multiply by $\exp(2\pi i/\lambda\ r.s_o)$).

– a-priori A, B, P calibrations applied to the model.

– use 3D global model to determine $G(t, s_0)$

– self calibration to determine $G(t, s_0)$ for each phase center.

– $G(t, s_0)$ measures tropospheric and ionospheric delays.

– $G(t, s_0, \nu, p)$ also includes corrections to A, B, P.

– calibrations are not independent for each phase center.

– SNR improved by global model of gain variations across array.

• Self calibration $\chi^2 = < \Sigma[V \times g_i g_j - V']^2 \ / \ \sigma_{ij}^2 >$

(summation over antenna pairs (i, j), frequency channels, time)

– χ^2 accumulated in distributed processors.

– calibration solves for gains g_i for each time interval and phase center.

• Calibrate data streams into beam formers and imagers.

– calibration needed at every level of beam formation.

– data streams delayed to interpolate calibration.

• SKA design and computing costs are strongly coupled.

– include cost of obtaining adequate image quality.

– high sidelobes, and coupling between beams increase computing costs.

– image quality is strong function of uv-coverage.

– correlator cost $\sim N^2/2$, but computing reduced by better uv-coverage.

10. COMPUTING and DATA PROCESSING MODEL

10.1. Stream Data Processing

• Survey research ideally suited to stream data processing.

– Calibration and Imaging implemented in close to real time.

– Delayed calibration and analysis limit science.

– Variable sources, Transients, and Targets of opportunity.

– RFI handled as the data are acquired.

– Off-line data reduction expensive and time consuming.

– Reduce burden of expert data reduction on the end user.

– Best use of telescope and human resources.

– Severe mismatch between on-line and off-line data processing rates.

– Calibrated images as standard output from SKA.

10.2. Data Rates.

• Total data bandwidth from the antennas:

$4\ 10^{12}\ (N/1000)\ (N_{pol}/2)\ (N_{beams})\ (B/GHz)\ (N_{bits}/8)$ bytes/s

• Channelize – Large N, BW, and RFI favor FX design.

– excellent separation of frequency channels using polyphase filter.

– RFI can be characterized using post correlation techniques.

– parallel data processing. Data rate reduced by N_{chan}.

• Data bandwidth at correlator

– sample correlator to make images over wide FOV.

– for siderial source anywhere in the entire sky:

$N(N+1)/2 \times N_{pol} \times N_{beams} \times N_{chan} \times N_{bits} \times 2\ sdot \times D_{max}/\lambda$

e.g. $N = 1000$, $N_{chan} = 10^5$, $N_{pol} = 4$, $N_{beams} = 1$, $D_{max} = 100\ km$, $\lambda = 10\ cm$, $N_{bits} = 2 \times 16$, *sdot* is earth rotation rate, $7.27\ 10^{-5}$ radian/s.

• Total data bandwidth $\sim 10^{14}$ bytes/s.

10.3. Integration at Multiple Phase Centers

• Images made simultaneously for multiple regions within FOV.

– data rate is reduced with further integration.

– FOV limited by primary beam, isoplanatic patch, array configuration.

• Data bandwidth for imaging primary beam $FWHM$ is:

$N(N-1)/2 \times N_{pol} \times N_{beams} \times N_{chan} \times N_{bits} \times 2\ sdot \times D_{max}/D_{ant}$

e.g. $N = 1000$, $N_{chan} = 10^5$, $N_{pol} = 4$, $N_{beams} = 1$, $D_{ant} = 12\ m$, $N_{bits} = 2 \times 16$

• Total data bandwidth $\sim\ 10^{12}$ bytes/s for 100 km baselines.

• Data rate per frequency channel $\sim$ 10 Mbytes/s.

– calibration and imaging within capabilities of modern PCs.

11. IMAGING

• Wide FOV Imaging is an iterative process.

– Forwards derivation of the sky brightness

– Deconvolution using the best model image.

– Deconvolution minimized by excellent uv coverage for large N.

– Calibration varies across FOV.

– Imaging optimized by maximizing data quality.

– Minimize instrumental parameters which must be determined.

• Parallel processing in distributed architecture.

– Subtract a-priori source model from calibrated uv data.

– Difference Images used to update the global model.

– Model and calibration improve as observations proceed.

• Observe until model image is consistent with uv data streams.

– 2D FFT used to image the region around each phase center.

– maximum image size for 2D FFT D_{max}/λ,

– $\sim 10^8$ beam areas on a 1000 km baseline at λ 1 cm.

– Variable sources are inconsistent with the global model.

– χ^2 image identifies transients.

• Imaging guided in real time by convergence of model and χ^2 image.

– Phase centers can be moved for science goals and calibration.

– Sources discovered in the imaging process.

– Adequately determine the calibration across the FoV.

– Model becomes the final image when observations are complete.

12. CONCLUSIONS

• Survey science requires low frequency, low resolution images with superb image quality, which imposes stringent requirements on the calibration and sidelobe levels at every stage of beam formation.

• The cost of data processing is very dependent on the antenna system, calibration, and science requirements. The optimal design of the SKA must consider the overall system from the science goals to the data products.

• The cost of the SKA is dominated by four major components: antennas, receivers, signal processing, and computing. Each has strong interdependencies, and must be optimized in the context of the overall science and engineering goals.

• Closer interactions between the astronomers and the engineers is essential to optimize the survey properties of the SKA. In some cases FOV can be traded for sensitivity but in many cases a large FOV is required at full sensitivity so there is no room to trade.

• Sources of non thermal noise may limit the capabilities of the SKA. For high dynamic range, sidelobes of sources outside the regions of interest must be subtracted or the SKA will be confusion limited. In order to achieve the sensitivity and image fidelity goals, the calibration must match the thermal noise.

• SKA surveys are all-sky imaging, and for the highest dynamic range will require all-sky calibration from a global model of the sky brightness and instrumental transfer function.

• The large frequency range, from 0.1 to 25 GHz requires multiple telescope apertures to provide cost effective large apertures at low frequencies, and precision antennas at high frequencies. LNSD is a good solution above $\sim$ 1 GHz transitioning from aperture arrays to small dishes with cooled receivers. Whilst a single dish provides good attenuation of emission outside its FOV, an aperture or dipole array has large, frequency and polarization dependent, sidelobes which couple beams across the sky.

• FPA receivers provide multiple beams to reuse the telescope aperture aperture and give a wider field of view, but transfer resources from collecting area to electronics which have short lifetime and higher replacement/maintenance costs.

• Array antennas, station beam formers and FPAs require careful calibration for high dynamic range observations. For the highest dynamic range the calibration implicit in beam-forming with FPA or station beams must be redone in the data analysis, which leads to a large increase in computing costs.

• The LNSD design maximizes ND for survey science. A LNSD array with single pixel receivers also maximizes the collecting area ND^2 for targeted observations. The instantaneous FOV requirement can be efficiently met above $\sim$ 1 GHz by using a large number of small, $\sim$ 5m, diameter antennas. Building a smaller number of larger antennas is not such a good solution since sources larger than the primary beamwidth must be mosaiced; the image fidelity is degraded by pointing errors and by the sparse *uv* coverage.

• Calibration and imaging are intimately related. We use a model of the sky brightness distribution to determine the instrumental and atmospheric calibrations. A model is used to subtract sidelobes from sources outside the regions of interest. The calibration varies across the sky due to uncertainties and time variations in the primary beam, instrumental polarization and non-isoplanicity. We must measure the gain variations in the directions of sources whose sidelobes corrupt the regions of interest. The calibration can be improved by using a global model of the sky brightness and gains.

• RFI is a serious problem. Self generated RFI from high speed digital electronics on the antennas must be carefully shielded. RFI and time variable sources must be identified and measured so they can be correctly separated and subtracted from the *uv* data.

• Extrapolating the existing deconvolution algorithms for off-line data processing of large fields of view is very expensive for a large N array. There is a severe mismatch between the data rates in the on-line correlator hardware and those supported by the off-line processing. These problems can be resolved by integrating the calibration and imaging into the data acquisition process

• Hardware and software demonstator projects serve as proof of concept where we discover what we really need to do to accomplish our goals.

Table 1: Limits on the Field of View and Sampling Rates for the ATA and SKA. D_{max} is the maximum antenna separation. D_{ant} is the antenna diameter. λ/D_{ant} is the primary beam FWHM. $sqrt(\lambda/D_{max})$ is the limit to the image size imposed by non-coplanar baselines. $N_f \sim \lambda D_{max}/D_{ant}^2$ is the number of image regions needed, using a 2D FFT, to cover the primary beam $FWHM$. c/D_{max} is an upper limit to the channel width to avoid bandwidth smearing on the longest baseline without delay tracking. $Fringe$ is the maximum rate of change of the cross correlation, and $Nyquist$ is the sample rate within the primary beam $FWHM$.

λ [m]	D_{max} [km]	D_{ant} [m]	λ/D_{max} [arcsec]	λ/D_{ant} [arcmin]	$sqrt(\lambda/D_{max})$ [arcmin]	N_f	c/D_{max} [kHz]	$Fringe$ [Hz]	$Nyquist$ [Hz]
1.00	1	6	206.26	572.9	108.7	27.8	300	0.07	0.02
0.21	1	6	43.32	120.3	49.8	5.8	300	0.35	0.02
0.03	1	6	6.19	17.2	18.8	0.8	300	2.42	0.02
1.00	1	12	206.26	286.5	108.7	6.9	300	0.07	0.01
0.10	1	12	20.63	28.6	34.4	0.7	300	0.73	0.01
0.01	1	12	2.06	2.9	10.9	0.1	300	7.27	0.01
1.00	10	12	20.63	286.5	34.4	69.4	30	0.73	0.12
0.10	10	12	2.06	28.6	10.9	6.9	30	7.27	0.12
0.01	10	12	0.21	2.9	3.4	0.7	30	72.7	0.12
1.00	100	12	2.06	286.5	10.9	694.4	3	7.27	1.21
0.10	100	12	0.21	28.6	3.4	69.4	3	72.7	1.21
0.01	100	12	0.02	2.9	1.1	6.9	3	727.	1.21
1.00	1000	12	0.206	286.5	3.4	6944.	0.3	72.7	12.12
0.10	1000	12	0.021	28.6	1.1	694.4	0.3	727.	12.12
0.01	1000	12	0.002	2.9	0.3	69.4	0.3	7270.	12.12
1.00	1000	25	0.206	137.5	3.4	1600.	0.3	72.7	5.82
0.10	1000	25	0.021	13.8	1.1	160.	0.3	727.	5.82
0.01	1000	25	0.002	1.4	0.3	16.	0.3	7270.	5.82

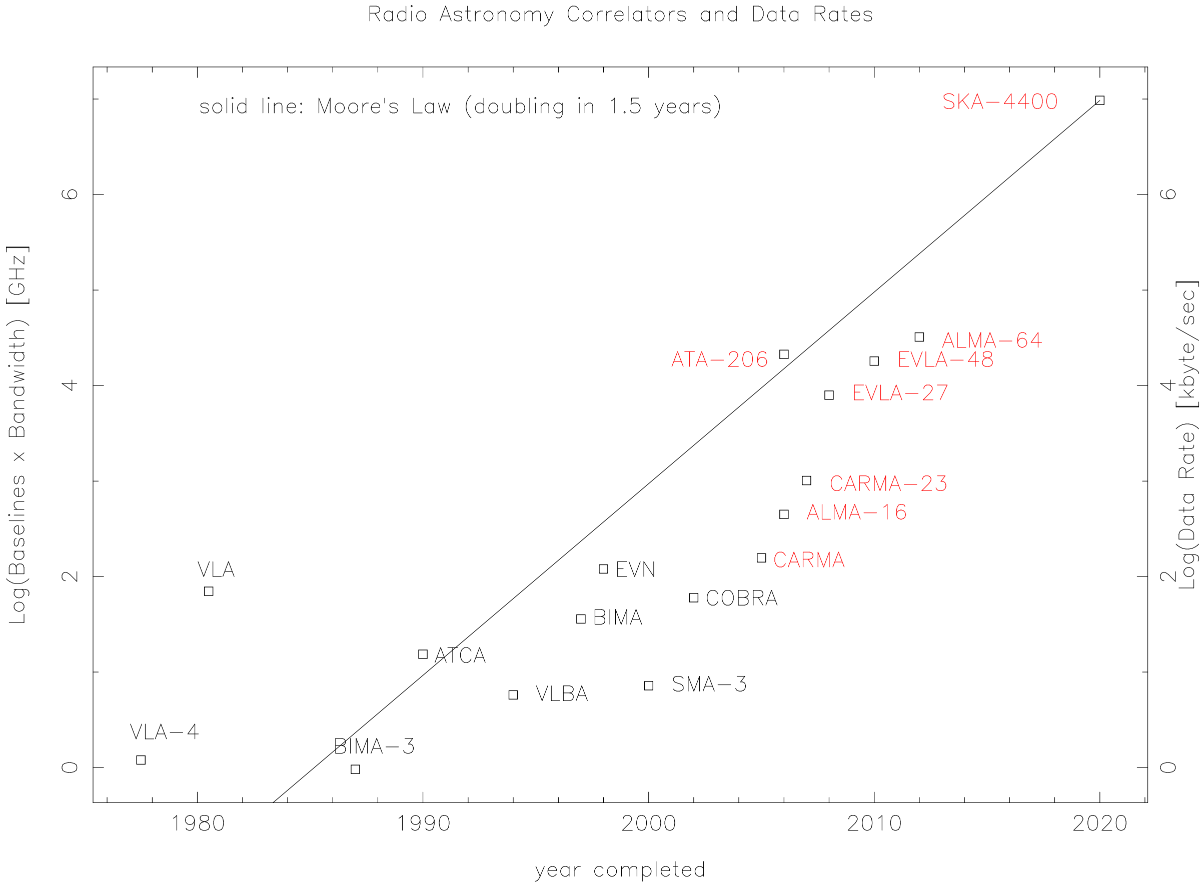

Fig. 1.— Radio Astronomy Correlators

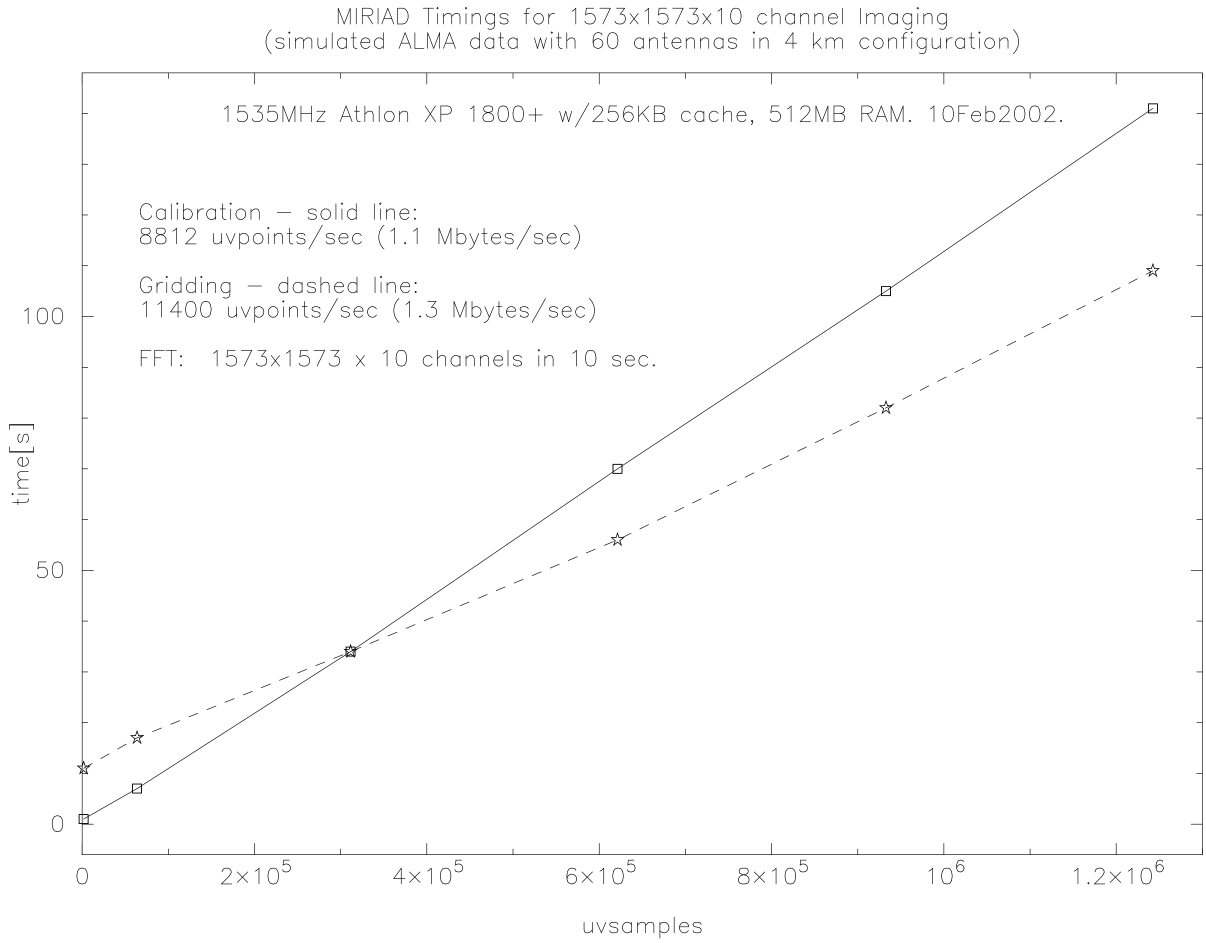

Fig. 2.— Multichannel Calibration and Imaging

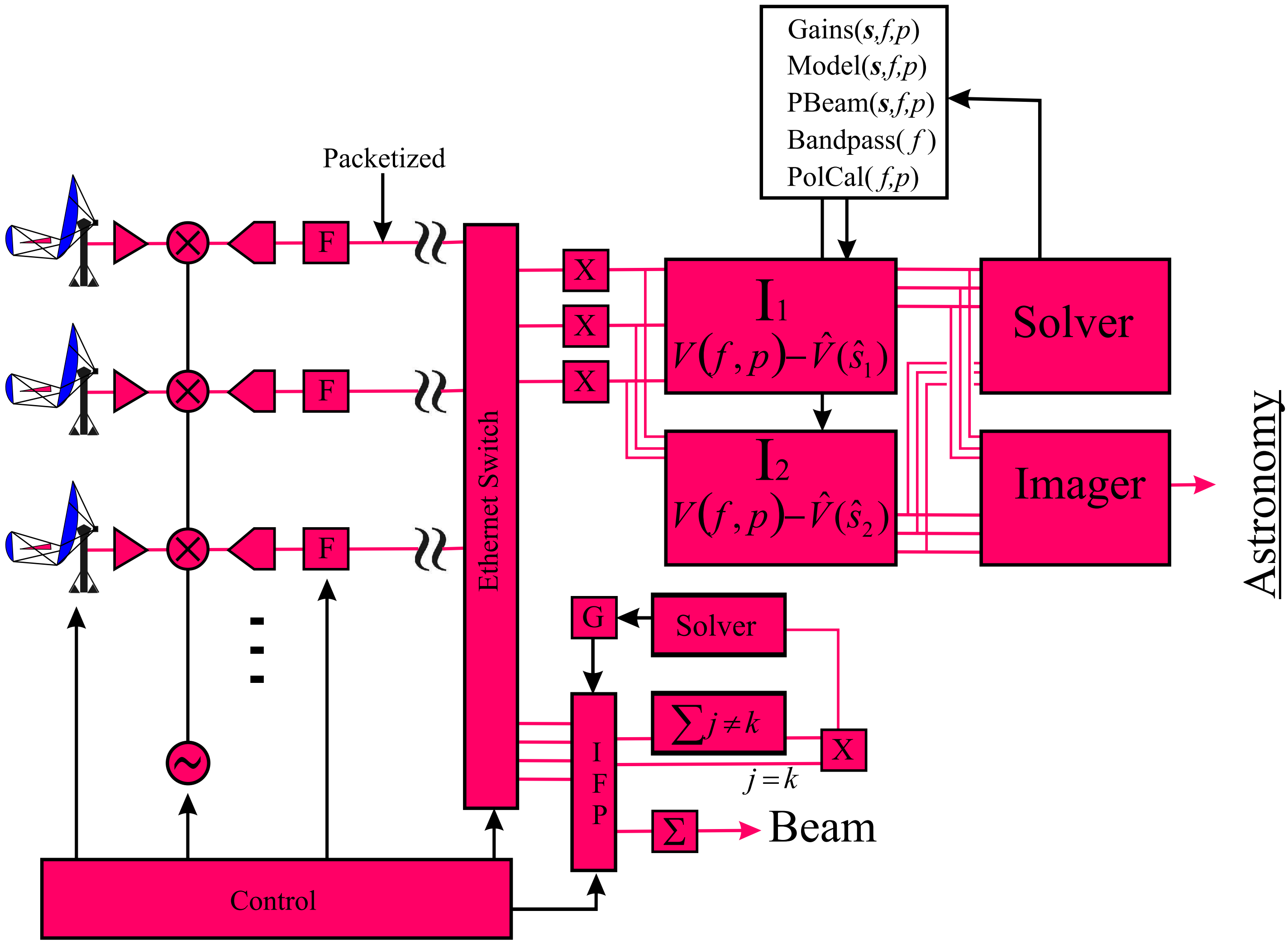

Fig. 3.— Data flow from telescopes to images. See text

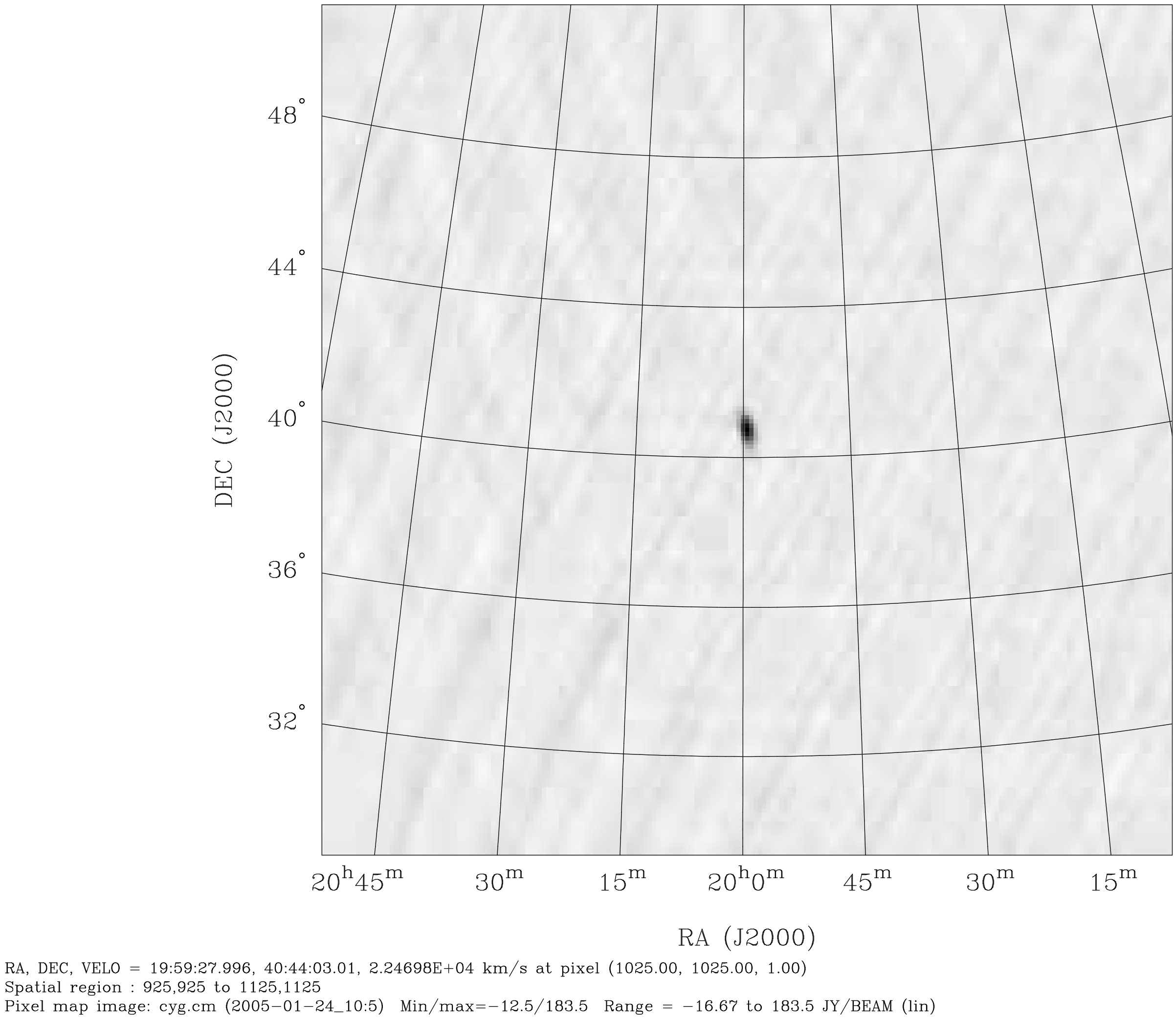

Fig. 4.— Cygnus Image at 175 MHz from 4-dipole array

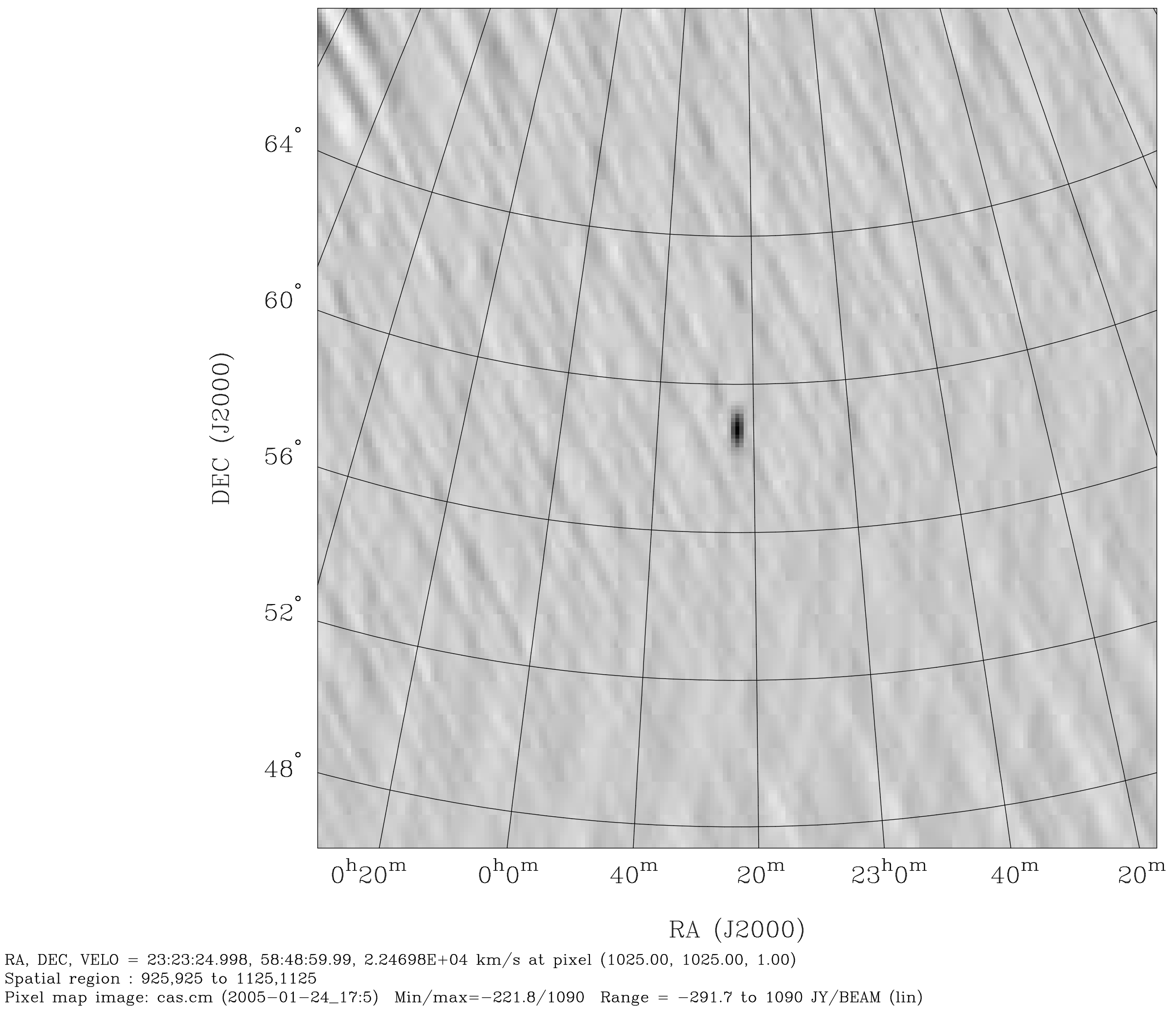

Fig. 5.— Cas A Image at 175 MHz from 4-dipole array

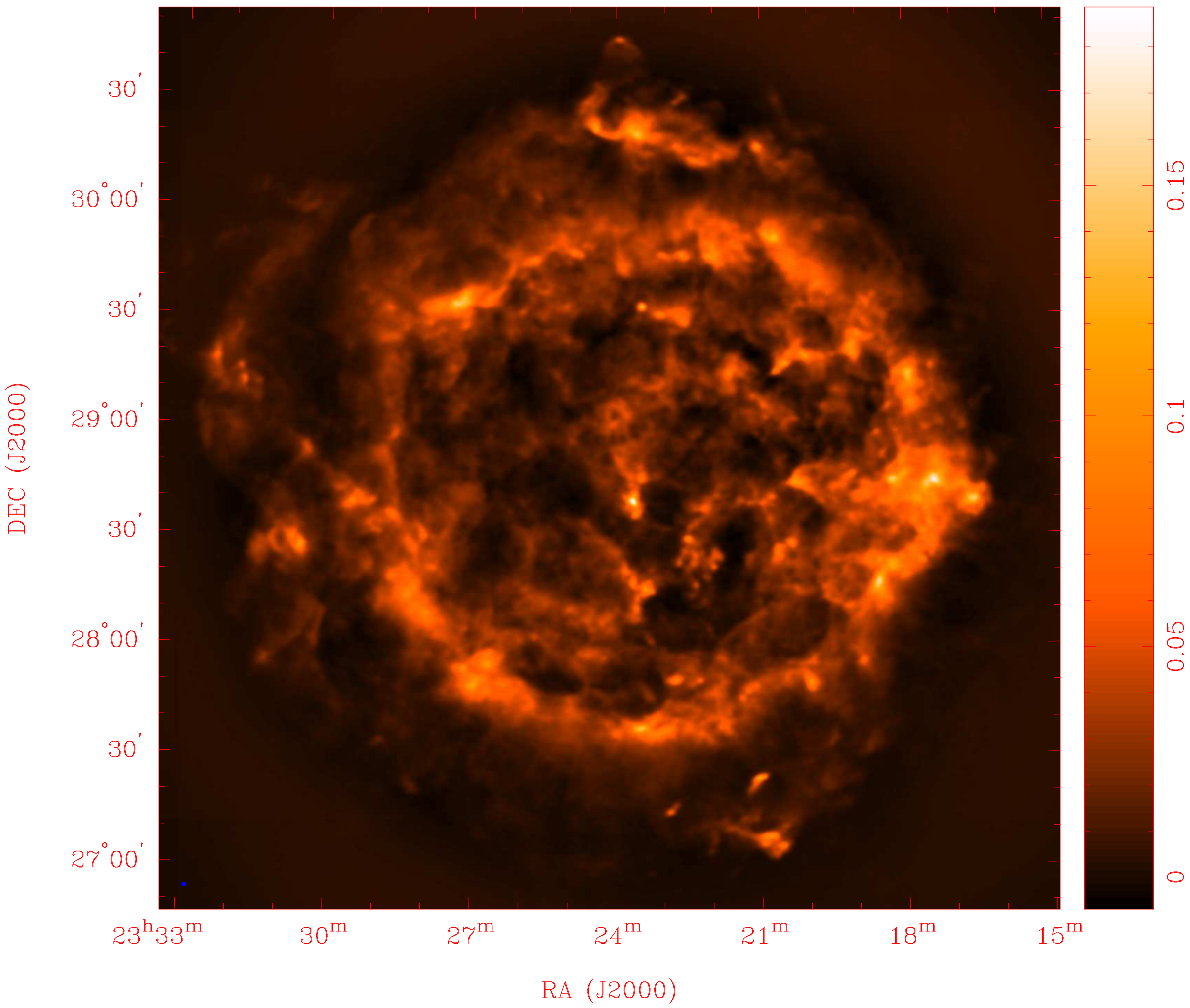

Fig. 6.— A mosaic MFS Image of CASA scaled up 40 times real size, imaged with the ATA at 1.42 GHz. The image is 4 degrees on a side. The synthesised beam FWHM, 77 x 78 arcsec is shown in the lower left corner.

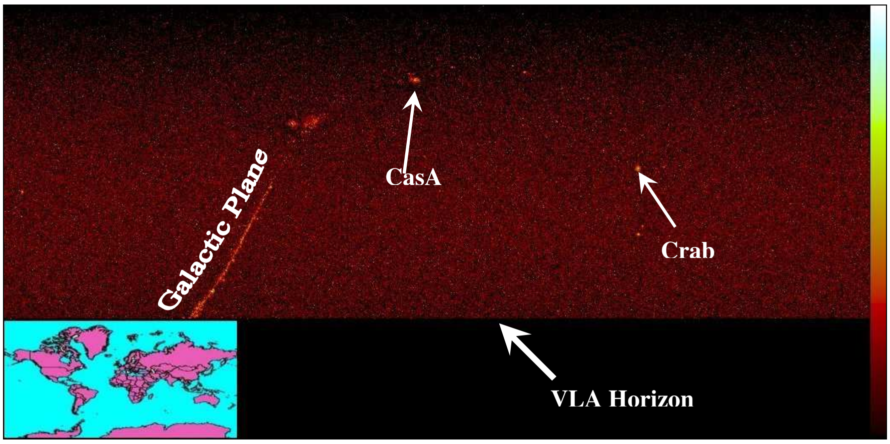

1

Fig. 7.— Mercator projection of NVSS survey at 1.4 GHz. Image center (RA,DEC) = (0,0). Left, right edges at RA = +/- 12 hours. Top, bottom edges at DEC = +/- 90 degrees. Color on log scale with Cas A at 0 db and spans 60 dB in power. INSET: Mercator projectionof world map for comparison. (Harp and Wright, 2006).

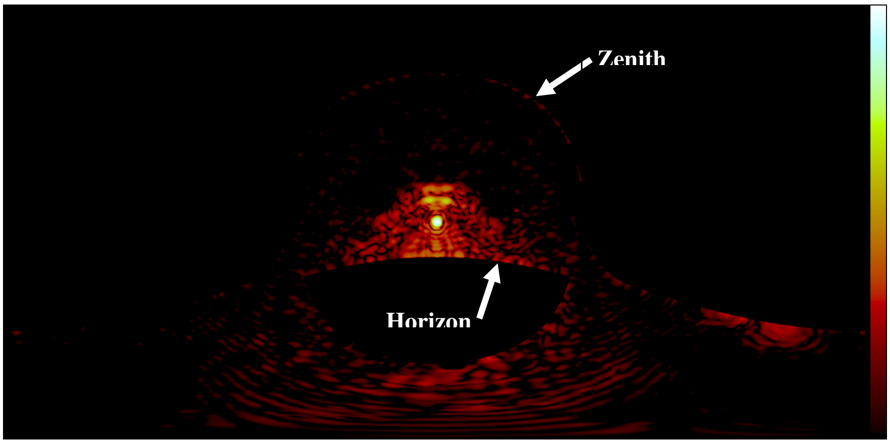

2

Fig. 8.— Mercator projection of ATA Primary beam pattern at 2.3 GHz. Image center (RA,DEC) = (0,0). Left, right edges at RA = +/- 12 hours. Top, bottom edges at DEC = +/- 90 degrees. Color on log scale from 0 db to -50 dB relative to beam maximum. Blank regions are not imaged due to pointing geometry. (Harp and Wright, 2006).

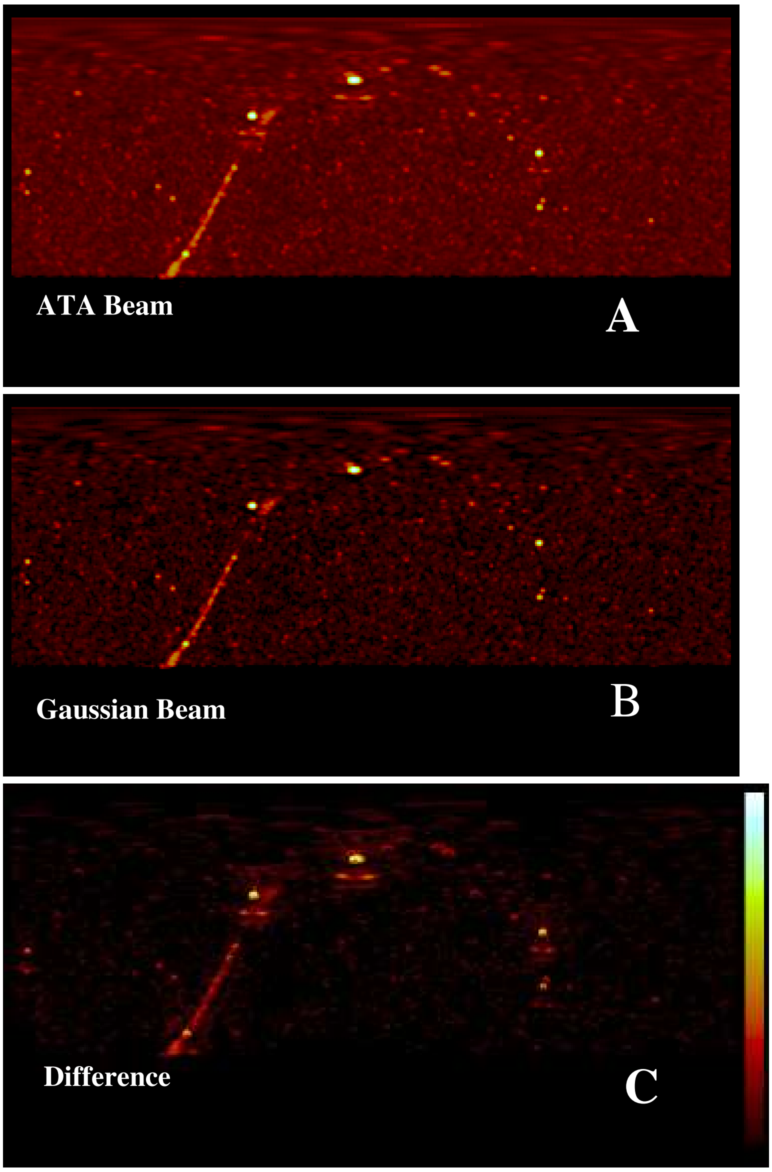

Fig. 9.— Simulations of NVSS survey convolved with (A) ATA primary beam, (B) Gaussian primary beam. (C) shows the difference image. Logarithmic scale spanning 30 dB. (Harp and Wright, 2006).

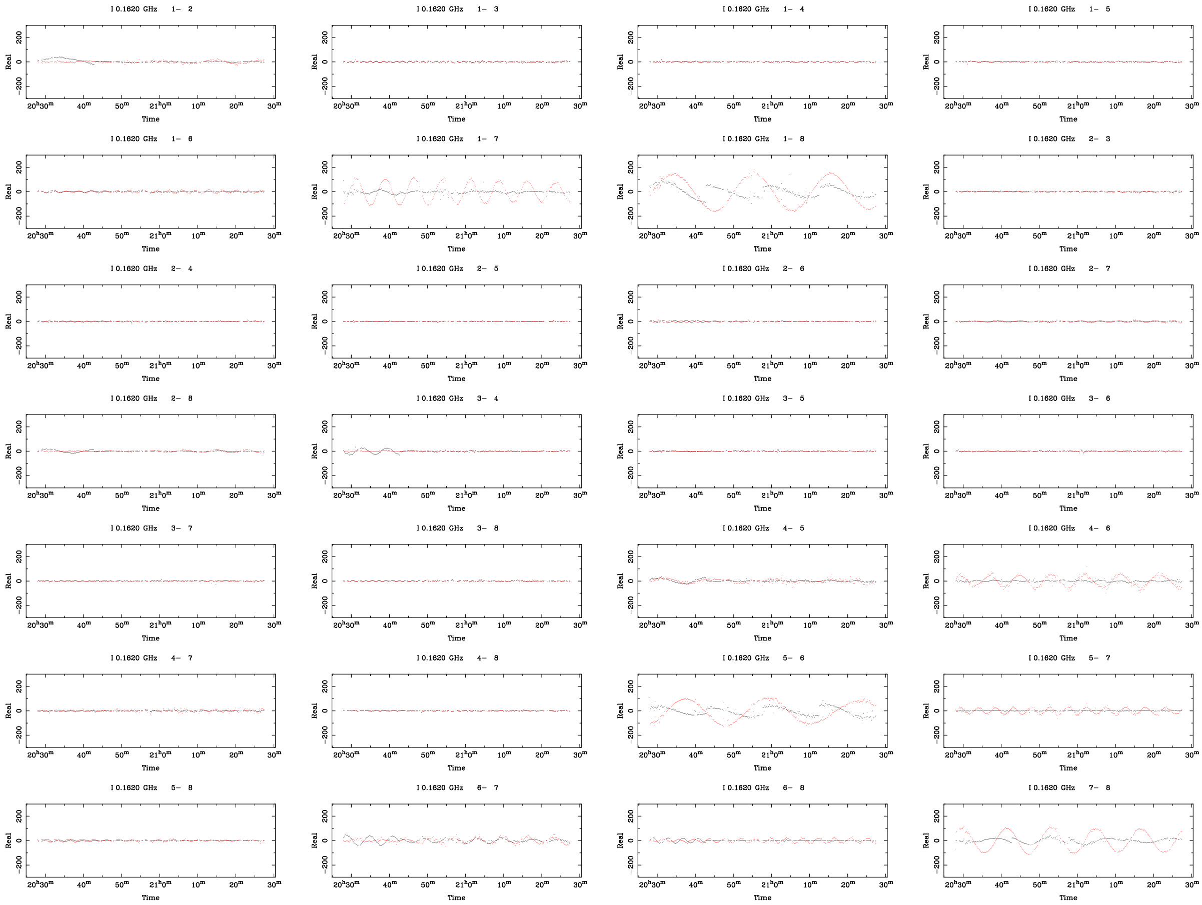

Fig. 10.— SUN subtraction from PAPER/GB 8-dipole array at 165 MHz. 300m diameter circle Cornwell-inspired, min-redundancy distribution. 7s per integration; 1h duration; 06jul27 data. *uvexsun* takes raw, zenith data (RA=LST,DEC=LAT), rotates to moving phase center of sun ($b.s$), averages for N minutes ($N = 15$) to get V_{sun}, returns to zenith data and removes $V_{sun} \times expi[b.s]$ on point by point basis. Figure plots before/after. Note that sun is resolved heavily in array. V_{sun} is (a) residual bx,by baseline fringe; (b) bz,tau and instrumental phase; (c) sun structure phase; (d) time variable sun. *uvexcat* will follow this approach removing a catalog of point sources, typically leaving one source for calibration step. In development stage next week or two.